Systematic and material independent variation of electrical, optical, and chemical properties of Ln-materials over the Ln-series (Ln=La,Ce,Pr,..,Lu)

Erik. van der Kolk, Pieter Dorenbos
Faculty of Applied Sciences, Delft University of Technology, Mekelweg 15, 2629 JB Delft,
The Netherlands

1. Abstract

A model is presented that successfully predicts electro-optical properties of Lanthanide materials, irrespective whether these materials are inorganic or organic, diluted or concentrated, metallic, semi-conducting or insulating. The model is firmly based on recent experimental data revealing that the variation in 4f and 5d energies relative to the valence band over the Ln series (La, Ce, Pr,.. ,Lu) is universal. Application to LnS and the oxides LnO, Ln_2O_3 and LnO_2 demonstrates its potential by correctly predicting the ground state electron configuration, metallic, insulating or semi-conducting behavior, Ln ion valence state and band-gap of these model Ln systems.

2. Introduction

Lanthanide (Ln) doped or concentrated materials are used in a diversity of applications such as lasers, light emitting diodes, phosphors or scintillators [*1*], and are being considered for future applications based on spintronics [*2*] or high density optical or magnetic data storage [*3*]. Besides application, Ln materials are at the focal point of solid state research into a variety of fundamental phenomena such as valence fluctuations [*4*], semi-conductor to metal phase transitions [*5*] or giant magneto resistance [*6*]. The wide variety of electrical, optical and magnetic behavior of Ln materials in both diluted and concentrated systems is to a large extend controlled by the energy of the 5d states relative to the 4f states. In wide band-gap insulators 5d states are well above the 4f ground state, and many luminescent materials are based on emissive transitions within the rich energy level structure of the 4f configuration [*7*]. When the lowest energy 5d states are close to, but still above, the 4f ground state, semi-conducting behavior dominates and ferromagnetic ordering with pronounced magneto-resistance effects has been observed [*6*]. When the lowest energy 5d state becomes resonant with the 4f ground state, Ln materials become critically sensitive to internal or external perturbations like pressure that can trigger a ground state configuration change from $4f^n5d^0$ to $4f^{n-1}5d^1$ resulting in a semi-conductor to metal phase transition and a non integer Ln ion valence state fluctuating in time [*8*]. Finally, integer Ln valence state and metallic behavior is observed when the lowest energy 5d state is well below the lowest energy 4f state.

Clearly, any model that has the pretension to explain and predict Ln material properties will need to consider the basic electronic structure, that is the ordering in energy of (i) the lowest energy Ln 4f state and (ii) the lowest energy 5d state, that is, the bottom of the 5d-derived conduction band (CB). In this report, we present experimental data convincingly demonstrating that the variation in energy of the 4f and 5d states relative to the valence band (VB) over the Ln series (La, Ce, Pr,.., Lu) in a particular material is independent of Ln valence state or concentration, and that

Optical Components and Materials IV, edited by Shibin Jiang, Michel J. F. Digonnet,
Proc. of SPIE Vol. 6469, 64690G, (2007) · 0277-786X/07/$18 · doi: 10.1117/12.698975

this variation is the same for inorganic or organic materials, metals, semi-conductors or insulators. This allows for the construction of a simple, easily applicable, phenomenological model that is highly effective in understanding and predicting basic Ln material properties like metallic or insulating behavior, lanthanide valences, nature and magnitude of the band-gap, or the stability of Ln materials. The model will be demonstrated by application to the well-known Ln mono-sulfides (LnS) and the Ln oxides LnO, Ln_2O_3 and LnO_2.

3. Experimental data on 4f and 5d energies of lanthanide ions

A considerable amount of experimental data on the energy of Ln 4f levels relative to the VB in materials exists, the majority of which is deduced from electron (XPS, UPS, XBIS) or optical spectroscopy (reflection, absorption, luminescence). Systematic studies providing the 4f energy of (almost) all Ln ions in the same material are only sparsely available. Lang *et al*. [*9*] established the energy of 4f levels of divalent and trivalent Ln ions in the Ln metals combining XPS and XBIS techniques. Thiel *et al*. [*10*] studied 4f energies relative to the VB using UPS in the garnets $Ln_3Al_5O_{12}$ for trivalent Ln ions ranging from Gd^{3+} to Lu^{3+}. Thompson *et al*. [*11*] studied the systematical behavior of 4f level energies of trivalent Gd, Dy, Er and Yb in organic complexes by XPS. Dorenbos followed a different approach and studied ligand to metal charge transfer (CT) energies of trivalent Ln ions as dopants in a wide variety of inorganic materials [*12*]. These CT energies of Ln^{3+} ions provide the location of the 4f ground state of Ln^{2+} ions above the VB [*13*]. Experimental data on the ground state 4f energy as a function of Ln ion relative to the VB are reproduced in the lower panel of Fig 1. The curves are shifted to zero energy at n=1 to compare the variation in energies of the different materials. It is immediately evident that the variation in energy over the Ln series is practically the same for all types of materials. Its double-seated form has been noticed before [*14*] and is similar to that of the free Ln ions except for an in-material Ln ion size dependent correction term [*15,16*]. Our conclusion is that this correction term is independent of the type of material, the Ln valence state or Ln concentration. A point to be stressed here is that once the position of the 4f level is known for one Ln ion in a specific material, the positions of the 4f level for all other Ln ions can be predicted for that material.

Experimental data on the energy of 5d states relative to the VB of each Ln ion in the same material do not exist. There is, however, a powerful indirect method to find those energies values by using the large volume of experimental data available on the energy of the 5d states relative to the 4f states of Ln ions as dopants. By adding this energy to the energies of the 4f levels, the location of the Ln 5d states are found. This method was adopted by Thiel *at al*. for the wide band-gap material $Ln_3Al_5O_{12}$ [*16*]. Experimental data on 4f→5d transitions, from the 4f ground state to the lowest energy 5d state, for di and trivalent Ln ions as dopants and in concentrated materials in a large number (>500) of materials ranging from highly ionic to covalent have been collected and analyzed by one of us [*17,18*]. An important conclusion of that work is that the variation over the Ln series in 4f→5d transition energy is independent of the type of host material, the Ln ion concentration and Ln valence state. This variation in energy is plotted in the top panel of Fig. 1 for the divalent and the trivalent cases (again curves have been shifted to zero energy at n=1) and shows a remarkable similarity to the inverse plot of the variation in the 4f energies (lower panel of Fig. 1). By adding the 4f→5d transition energies to the 4f energies, i.e., adding the values in the upper and lower panels in Fig. 1, we get the variation in energy of the lowest 5d states across the Ln

series for all materials. The result is indicated by the ● symbols in Fig. 1, which shows that the change in energy of the Ln 5d states over the Ln series for any specific material is constant to within 0.5 eV which is considered as the typical experimental error in the electron or optical spectroscopy data discussed above.

4. A model predicting electro-optical properties of Lanthanide materials

The universal behavior of the 4f and 5d energies relative to the VB, irrespective the type of material, the Ln valence state or Ln concentration, allows one to extrapolate VB, 4f and 5d energies and corresponding electro-optical properties of all the Ln ions in a specific material when the properties of only one Ln ion in that material have been established. This opens up the possibility of constructing a simple but highly effective phenomenological model that is illustrated in Fig. 2 where it is applied to the Ln mono-sulfides. The left panel of Fig. 2 schematically represents the density of states of EuS. The ligand 3p-derived VB, the localized $4f^7$ ground state and the 5d-derived CB band (split into a $5dt_{2g}$ and $5de_g$ state in the cubic crystal field of EuS) are plotted. Their relative energies are firmly established and were taken from the data of Wachter [*19*]. The dashed lines connect the top of the VB, the lowest energy $4f^7$ and 5d state of EuS to the right panel of Fig. 2 where they are represented by a square, triangle and circle, respectively, at n+m=7. Here we have adopted the common notation $4f^n5d^m$ for the electron configuration of the Ln ion. The model predicts that the 5d states of the other Ln ions will have the same energy relative to the VB and that the lowest energy 4f states follow the double seated shape, as shown. It follows that the ground state electron configuration and valence state of all the Ln sulfides are correctly reproduced. The $4f^{n-1}5d^1$ to $4f^n5d^0$ ground state configuration crossover, and the corresponding metal to semi-conductor transition, in the first half of the Ln series is predicted between Pm and Sm and between Tm and Yb for the second half. Only EuS and YbS are semi-conductors with a small gap between the 4f and 5d states. For the other Ln sulfides it is energetically more favorable to delocalize one 4f electron per Ln ion in the lower energy 5d state resulting in a metallic phase with predominantly trivalent Ln ions. The model appears sufficiently accurate to predict critical behavior for SmS and TmS with resonant 4f and 5d states (see Fig. 2). Indeed SmS has earned certain notoriety due to its unique iso-structural first order semi-conductor to metal phase transition at only a modest pressure of 6.5 kbar [*20*]. TmS has metallic properties with integer (3+) valence at low temperature but becomes mixed valence at ambient conditions [*21*].

5. Systematic behavior of the electro-optical properties of LnO, Ln_2O_3 and LnO_2

The full potential of the model for Ln materials is demonstrated by applying it to the Ln oxides LnO, Ln_2O_3 and LnO_2. These oxides were chosen for their wide variety of electro-optical properties that cannot be explained easily. They are also model substances in "ab initio" theoretical modeling [*22*]. We will show that our model correctly predicts valence states, metallic, insulating or semi-conducting behavior, band-gaps and the existence or non-existence of these three oxide systems.

Fig. 3A organizes the electronic structures of the Ln mono-oxides (LnO), a system of which EuO has received by far the most attention because of a pronounced semi-conductor to metal phase transition below the magnetic ordering temperature [*6*]. Using detailed experimental work available for EuO [*6,19*] the $4f^7$ ground state

of Eu^{2+} is placed 1.2 eV below the empty lowest energy 5d state. The VB maximum is placed 3.8 eV below the 4f state [*23*]. This is sufficient information to position the lowest energy 4f and 5d states relative to the VB for the other LnO's. Much in analogy to the LnS system our model predicts a ground state configuration change when going from La to Lu over the Ln series when the 4f energy drops below the 5d energy. For EuO and YbO (white area's), electrons no longer occupy the 5d CB but are localized in the 4f state resulting in a valence change from Ln^{3+} to Ln^{2+} and a small band-gap close to 1 eV. For the other Ln oxides the electron is delocalized over the 5d CB and metallic behavior is observed (shaded area's). Our model correctly predicts the ground state configuration, the Ln ion valence state and the conduction behavior, including that of SmO whose electronic properties critically depend on the relative positioning of the 4f and the 5d energies. Indeed SmO is metallic [*24*]. TmO should be metallic like SmO.

Figure 3B represents the electronic structure of the sesquioxides Ln_2O_3 (hexagonal structure type) as derived by our model. The relative position of the three curves in Fig. 3B is set by the well-established band-gaps of La_2O_3 (2.4 eV) and Ce_2O_3 (2.4 eV) [*25*] that are defined by a VB→5d(CB) and a 4f→5d(CB) transition for La_2O_3 and Ce_2O_3 respectively. Based on these two easy obtainable experimental values, the lowest energy 4f and 5d states of all the other Ln ions are established. Our model correctly predicts, well within the experimental error of 0.5 eV, the nature and the variation in the band-gap over the Ln series as shown by the colored area in Fig 3B. It follows that for La, Pm, Sm, Gd, Ho, Er, Tm and Lu, the nature of the band-gap is the same as for La_2O_3. Smaller band-gaps are predicted and found for the Ln ions with occupied 4f levels above the VB. In those cases (Ce, Pr, Nd, Tb and Dy) gaps are defined by a 4f→5d(CB) transition as was the case for Ce_2O_3 .

Besides VB→5d(CB) and a 4f→5d(CB) transition, a transition from the VB to the 4f state needs to be considered. Since such a transition ends in the 4f ground state of the Ln^{2+} ion ($Ln^{3+}+e\rightarrow Ln^{2+}$), the double-seated curve of the (unoccupied) 4f states of Ln^{2+} ions in Ln_2O_3 is included in Fig. 3b (Unfilled Δ symbols). This curve is placed relative to the VB by using the CT energy of Eu^{3+} as dopant in Gd_2O_3 [*26*]. The in this way predicted band-gap values of Eu_2O_3 and Yb_2O_3 compare well with the measured values.

Finally the Ln di-oxides (LnO_2) are considered in Fig 3C. No information is available on the energy of the 4f and 5d states of Ln^{4+} ions relative to the VB in these di-oxides. The only well established experimental fact is a 3 eV, CT energy from the VB to Ce^{4+} in CeO_2 [*27*]. Since this VB→4f transition ends in the 4f ground state of the Ce^{3+} ion, the double-seated curve representing the (unoccupied) 4f states of the Ln^{3+} ions in LnO_2 is drawn in Fig. 3C (unfilled Δ symbols). This curve shows that the unoccupied 4f state drops into the VB twice, once in the first half of the Ln series and once in the second half. Since empty levels below the top of the VB cannot exist, they must be occupied so that the trivalent Ln state is preferred and the LnO_2 phase (with Ln^{4+} ions) does not exist. According to our model this is the case for Pm to Gd and from Ho to Lu as indicated by the white areas in Fig 3c. In practice however, the unoccupied Ln^{3+} 4f levels stay unoccupied only when they are significantly above the VB maximum. Indeed, among the Ln dioxides, only CeO_2, PrO_2 and TbO_2 have been synthesized successfully [*28*]. It is interesting to observe the close similarity between the electronic structure between these three oxide systems (compare Fig. 3A, B and C), only the filling of 4f and 5d states is different.

We emphasize that the above analysis is not limited to the binary Ln oxides but is also successful when applied to other Ln chalcogenides, pnictides and halides

other than binary. It is especially interesting to apply the model to materials not yet fully investigated or understood.

6. Conclusions

In conclusion, we have presented experimental data showing that the variation in energy of the 4f and 5d states relative to the VB over the Ln series is independent of the type of Ln material. This forms the basis of a phenomenological model capable of predicting the energy of all the Ln ion 4f and 5d states with respect to the VB, once experimental data on one of the Ln ions is available. The model successfully predicts basic electro-optical properties of LnS, LnO, Ln_2O_3, and LnO_2, but can be applied to any Ln material. It may serve as a reliable tool for material scientist and may accelerate design of a broad range of Ln materials with deliberately chosen properties.

7. References

[1] S. Shionoya, W.M. Yen, *Phosphor Handbook* (CRC Press, New York, 1998).
[2] P. LeClair *et al*., *Appl. Phys. Lett*. **80**, 625 (2002).
[3] S. Tsunashima, *J. Phys. D*, **34** (17) 87 (2001).
[4] P. Strange, A. Svane, W.M. Temmerman, Z. Szotek, H. Winter, *Nature*, **399** 756 (1999).
[5] P. Wachter, *Handbook on the Physics and Chemistry of Rare Earths* (Elsevier, Amsterdam, 1994, Vol. 19, Chap. 132).
[6] P. G. Steeneken *et al*., *Phys. Rev. Lett*. **88** (4) 047201 (2002).
[7] C. R. Ronda, *J. Alloys Compd*. **225**, 534 (1995).
[8] J.M. Lawrence, P.S. Riseborough, R.D. Parks, *Rep. Prog. Phys*. **44** (1) 1 (1981)
[9] J.K. Lang, Y. Baer, *Phys. Rev. Lett*. **42** (1) 74 (1979).
[10] C.W. Thiel *et al*., *Phys. Rev.* B **64**, 085107 (2001).
[11] J. Thompson *et al*., *Phys. Rev.* B **70,** 153104 (2004).
[12] P. Dorenbos, *J. Phys. Cond. Matter* **15,** 8417 (2003).
[13] W.C. Wong, D.S. McClure, S.A. Basun, M.R.Kokta, *Phys. Rev. B* **51,** 5682 (1995).
[14] J.A. Wilson, *Structure and Bonding* **32,** 58 (1977).
[15] C. Pedrini, D.S. McClure, C.H. Anderson, *J. Chem. Phys*. **70** (11) 4959 (1979).
[16] C.W. Thiel *et al*., *J. Lumin*. **94-95**, 1 (2001).
[17] P. Dorenbos, *J. Lumin*. **91**, 91 (2000).
[18] P. Dorenbos, *J. Phys. Cond. Matter* **15,** 575 (2003).
[19] P. Wachter, *Critical reviews in Solid State Science* **3**, 189 (1972).
[20] A. Jayaraman, V. Narayanamurti, E. Bucher, R.G. Maines, *Phys. Rev. Lett*. **25**, 1430 (1970).
[21] P. Wachter, S. Kamba, M. Grioni, *Physica B* **252,** 178 (1998).
[22] L. Petit, A. Svane, Z. Szotek, W.M. Temmerman, *Phys. Rev.* B **72**, 205118 (2005).
[23] N. Yamashita, *J. Lumin*. **59,** 195 (1994).

[24] J.M. Leger, P. Aimonina, J. Loriers, P. Dordor, B. Coqblin, *Phys. Lett*. **80** (4) 325 (1980).
[25] A.V. Prokofiev, A.L. Shelykh, B.T. Melekh, *J. Alloys Compd*. **242,** 41 (1996).
[26] G. Blasse, *J. Electrochem.: Solid state Sci*. **114**, 875 (1967).
[27] F. Marabelli, P. Wachter, *Phys. Rev.* B **36** (2) 1238 (1987).
[28] G.Y. Adachi, N. Imanaka, *Chem. Rev*. **98,** 1479 (1998).
[29] This work was supported by the Dutch Technology Foundation (STW).

Figure 1

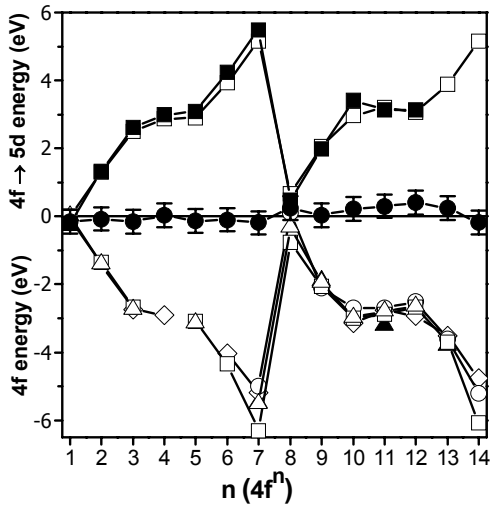

(Top panel) Variation in energy of the lowest energy 4f→5d transition over the Ln series of Ln^{2+} (□) and Ln^{3+} (■) impurities in inorganic insulators and semi-conductors. (bottom panel) Variation in energy of the lowest energy 4f state relative to the VB of Ln^{2+} (Δ) and Ln^{3+} (□) ions in Ln metals, Ln^{3+} ions in $Ln_3Al_5O_{12}$ (○), Ln^{3+} ions in organic complexes (▲) and of Ln^{3+} impurities in inorganic insulators and semi-conductors (◇). The ● symbols represent the calculated variation in energy of the lowest energy 5d states.

Figure 2

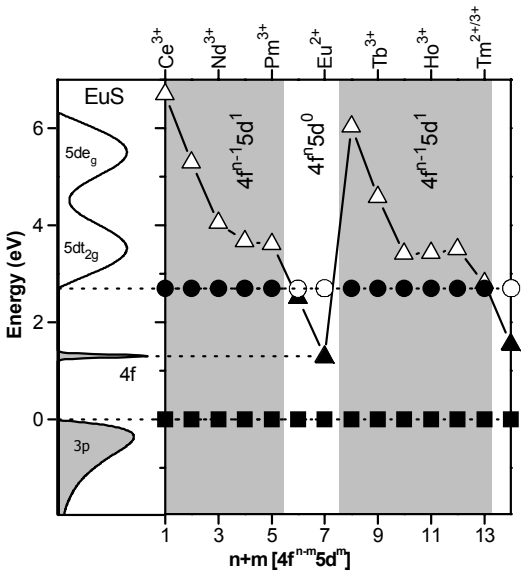

Figure 2. EuS density of states and the predicted variation over the Ln-series (La,Ce,Pr,..,Lu) of the electronic structure of the LnS. (left panel) Schematic representation of the density of states of the sulphur 3p-derived VB, the localized Eu $4f^7$ ground state and Eu 5d-derived CB in EuS. (right panel) Predicted variation in energy over the Ln-series of the VB maximum (□), the lowest energy $4f^n$ (Δ) and $4f^{n-1}5d^1$ (○) states for the Ln mono sulphides. Filled symbols refer to occupied states. Coloured areas represent Ln-sulphides with metallic properties with a $4f^{n-1}5d^1$ electron configuration. Gray areas indicate semi-conducting Ln-sulphides for which it is energetically more favourable to localize one electron per Ln-ion in the 4f shell resulting in a $4f^n5d^0$ configuration.

Figure 3

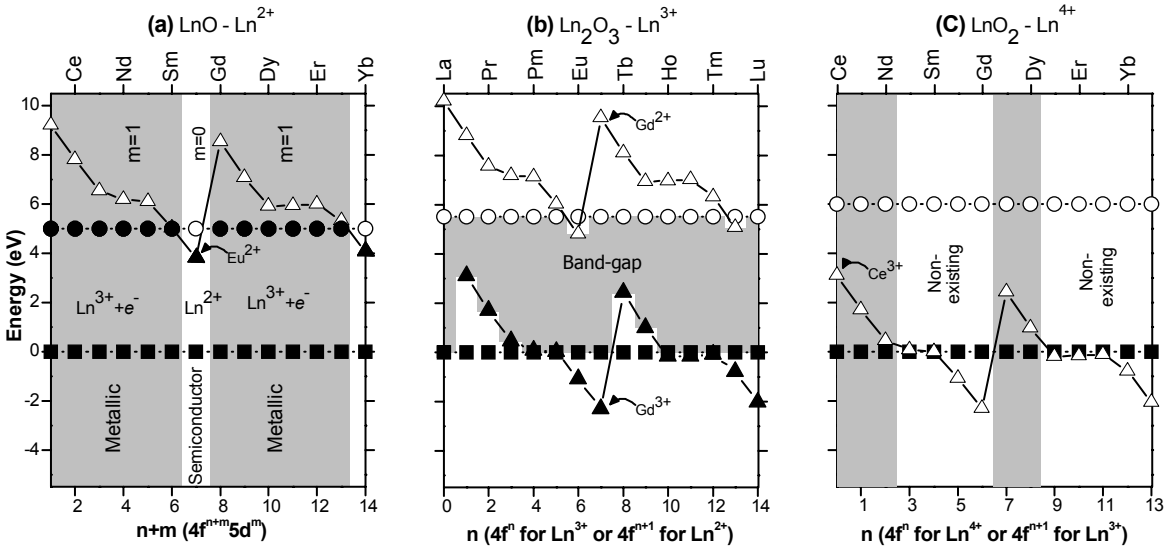

Figure 3. Predicted variation over the Ln-series (La,Ce,Pr,..,Lu) of the electronic structure of the binary Ln-oxides. The VB maximum (□), the lowest energy 4f (Δ) and 5d (○) states are indicated by filled or open symbols representing occupied or unoccupied states respectively. Based on minimal experimental data our model correctly predicts (panel **a**) semi-conducting or metallic behaviour as well as valences and valence changes of Ln-ions for the LnO, (panel **b**) the nature and magnitude of band-gap energies for the Ln_2o_3 and (panel **c**) the chemical stability of the LnO_2.